PHYSICAL REVIEW C VOLUME 33, NUMBER 3 MARCH 1986

Test of the triaxial rotor model and the interacting boson fermion approximation model description of collective states in ^{191}Ir

F. K. McGowan, N. R. Johnson, I. Y. Lee, W. T. Milner, C. Roulet,* J. Hattula,† M. P. Fewell,‡ and Y. A. Ellis-Akovali
Oak Ridge National Laboratory, Oak Ridge, Tennessee 37831

R. M. Diamond and F. S. Stephens
Lawrence Berkeley Laboratory, Berkeley, California 94720

M. W. Guidry
University of Tennessee, Knoxville, Tennessee 37916 and Oak Ridge National Laboratory, Oak Ridge, Tennessee 37831
(Received 29 July 1985)

Coulomb excitation of states in ^{191}Ir up to $J=\frac{21}{2}$ has been observed with 160-MeV ^{40}Ar and 617-MeV ^{136}Xe ions. Most of these states are grouped into three rotational-like bands based on the $\frac{3}{2}^+$ ground state, the $\frac{1}{2}^+$ first excited state, and the $\frac{7}{2}^+$ γ-vibrational-like state at 686 keV. The average deviation between experimental and theoretical energies for 20 states is 45 keV for the particle-asymmetric-rigid-rotor model and 125 keV for the interacting boson fermion approximation model [limited to broken Spin(6) symmetry, and only the $d_{3/2}$ orbital is considered]. The overall agreement of both model predictions with experimental γ-ray yields for transitions within the $\frac{3}{2}^+$ band is quite good. For interband transitions originating in the $K=\frac{1}{2}^+$ and $\frac{7}{2}^+$ bands, the interacting boson fermion approximation model tends to underestimate the γ-ray yields by one to two orders of magnitude. These six moderately collective transitions correspond to $\Delta\tau_1=2$ transitions in the U(6/4) and U(6/20) supersymmetry schemes and are strictly forbidden in these schemes. For both supersymmetric schemes there is a lack of detailed agreement with the very collective $E2$ transitions which have $\Delta\tau_1=0,\pm1$. The triaxial rotor model description of the experimental energies and the collective $E2$ transitions is the most successful approach. The $B(E3)$ for excitation of several negative-parity states in ^{191}Ir is $(4\pm1)B(E3)_{\rm sp}$.

I. INTRODUCTION

The Os and Pt nuclei are in the prolate to oblate shape-transition region. Several different collective models have accounted for properties of their lowest-lying states with varying degrees of success. These models range from the asymmetric rigid rotor through various rotation-vibration models about triaxial and axial shapes to the γ-unstable (shape-unstable) model. Kumar and Baranger have done collective-model calculations within the framework of Bohr's collective Hamiltonian. The potential-energy surfaces and inertial parameters are derived microscopically by using the pairing-plus-quadrupole model of residual interactions.[1] These calculations predict a prolate to oblate shape transition in the Os and Pt nuclei and also potential-energy surfaces with shallow minima, especially soft to γ vibrations.

Lee *et al.*[2] Coulomb-excited the ground-state band up to $J^\pi=10^+$ and the γ-vibrational-like band up to $J^\pi=8^+$ in ^{192,194,196}Pt with ^{136}Xe projectiles. The observed γ-ray yields imply $B(E2)$ values which follow the asymmetric-rigid-rotor model predictions. An analysis[3] of unique parity energy-level spectra based on high-j negative-parity orbitals in adjacent unstable odd-A nuclei with the rigid-triaxial-rotor-plus-particle model reveals values of the deformation parameter γ in the range $20°<\gamma<35°$.

The collective properties of low-lying states in even-even nuclei can be described with moderate success in the framework of the interacting boson model (IBM) of Arima and Iachello.[4–6] The states of this model are classified according to the symmetric representations $[N]$ of the group SU(6), where N is the number of bosons. The O(6) subgroup[6] of the group SU(6) for $N\to\infty$ corresponds to the γ-unstable nucleus of the geometrical model.[7]

More recently the IBM has been extended to odd-A nuclei by coupling a single fermion to the even-even core.[8] This approach is referred to as the interacting boson-fermion approximation (IBFA) model. Whenever the core Hamiltonian possesses one of the dynamical symmetries, the corresponding odd-A energy level spectra exhibit simple features.[9] The O(6) symmetry is considered here since it is applicable to nuclei in the shape-transition region. The features of the odd-A energy-level spectra[9] in the interacting boson-fermion model (IBFM) are analogous to those of the particle-plus-γ-soft-rotor model.[10]

Iachello also proposed that dynamical supersymmetries[11] may be present in the energy-level spectra of complex nuclei. This suggestion was based on the analysis of the energy-level spectra of the pair of nuclei ^{192}Pt and ^{191}Ir, in which the states of the combined system of bosons and fermions can be simultaneously classified within the same group-theoretical framework. Since then, considerable theoretical effort has gone into developing this idea. As a result, two types of symmetries, spinor[12] symmetries and supersymmetries,[13] have been found which may be useful in classifying the level spectra of certain even-A and odd-A nuclei. In particular, Spin(6) symmetry and U(6/4) supersymmetry may be evident in the Os-Ir-Pt nuclei. The isotopes of Os, Ir, and Pt constitute an ideal testing ground for these proposed symmetries. An analysis of the experimental evidence, excitation energies, and reduced E2 transition probabilities, for ^{190}Os, ^{191}Ir, ^{192}Os, and ^{193}Ir has already been presented by Balantekin *et al.*[13] This limited experimental evidence lends support to the suggestion that supersymmetry may occur in these nuclei.

Perhaps the most successful interpretation of the $^{187-193}$Ir positive parity states is the particle-asymmetric-rigid-rotor model.[14] In this model several Nilsson orbitals are coupled to a rigid asymmetric core. Each Nilsson orbital represents a superposition of several shell model configurations. Coupling the Nilsson orbital to an asymmetric core further complicates the wave function of each state. Instead of a single band built on a Nilsson orbital as would be the case of an axially symmetric core, several "rotational" bands result which can be labeled by a quantum number K of the main component in their wave functions. The analysis by Vieu *et al.*[14] also provided a satisfactory description of the reduced $E2$ transition probabilities available from light-ion Coulomb excitation of ^{191,193}Ir.

We have used Coulomb excitation with heavy ions to enhance the multiple-step process in ^{191,193}Ir and determined properties of higher-spin states in these two nuclei. In this paper we present the results from Coulomb excitation of ^{191}Ir and compare the results with the predictions of two models, viz., the particle-asymmetric-rigid-rotor model and the IBFA model. These results also test the role of supersymmetry in this mass region.

II. EXPERIMENTAL PROCEDURE AND RESULTS

We have observed Coulomb excitation of states up to $J=\frac{21}{2}$ with 617-MeV ^{136}Xe ions from the SuperHILAC and 160-MeV ^{40}Ar ions from the Oak Ridge isochronous cyclotron (ORIC). At the SuperHILAC the γ rays from Coulomb excitation were detected in two Ge(Li) detectors located at 92.6° and −149.2° and at distances of 8.1 and 8.9 cm from the target, respectively, in coincidence with scattered projectiles and recoiling nuclei. These particles were detected in two parallel plate avalanche counters

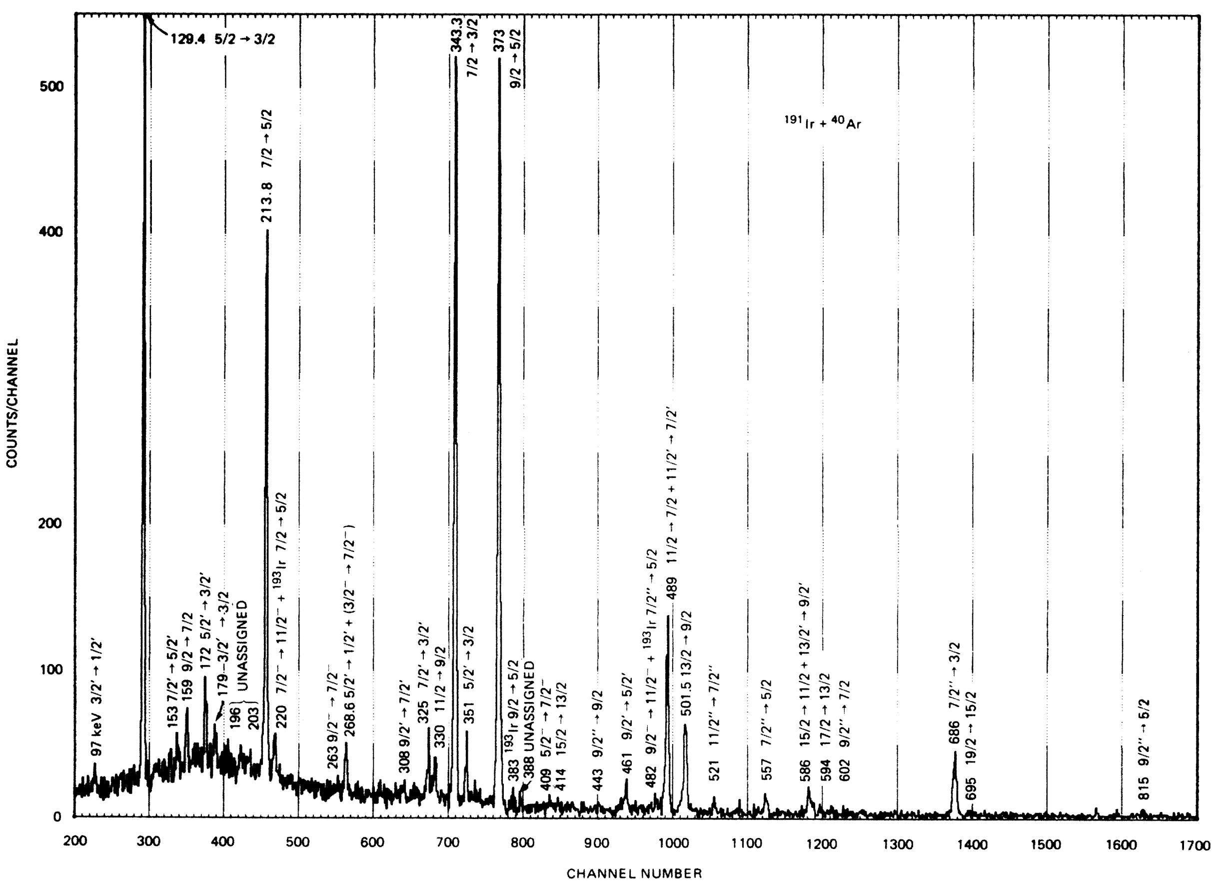

FIG. 1. Gamma-ray spectrum observed at 0° from Coulomb excitation of ^{191}Ir with 160-MeV ^{40}Ar ions. The label above each peak is the transition energy and transition assignment. The unprimed, single-primed, and double-primed states refer to states in the $\frac{3}{2}^+$, $\frac{1}{2}^+$, and $\frac{7}{2}^+$ rotational-like bands, respectively.

(PPAC's) 12 cm×12 cm located at 26.5° and −83.5° and at a distance of 18 cm from the target. The larger scattering angle corresponds to $\theta_{c.m.}=128°$. An array of six NaI detectors was placed around the chamber to provide multiplicity information with each event. The Doppler broadening of the γ-ray lines was minimized by using a thin target and placing the Ge(Li) detector in the average recoil direction of the ^{191}Ir nuclei. The γ-ray detection efficiency of the Ge(Li) detectors was determined using a calibrated ^{152}Eu source.

At ORIC the backscattered ^{40}Ar ions were detected in an annular solid-state surface-barrier detector which extended from 154° to 171°. Gamma rays in coincidence with backscattered ^{40}Ar were detected in three Ge(Li) detectors located at $\theta_\gamma=0°$, 55°, and 90° with respect to the ion beam and at distances of 7 to 13 cm from the target. An isotopically enriched (98.17% ^{191}Ir) target 1.0 mg/cm^2 thick on 0.51×10^{-6} m Ni was prepared by a focused-ion-beam sputtering system. Doppler broadening of the γ-ray lines was minimized by allowing the excited nuclei to recoil out of the target and decay in flight. The beam was stopped in a Pb foil 2 cm downstream from the target.

Figure 1 shows a coincidence γ-ray spectrum of ^{191}Ir after subtraction of the random counts. The label above each peak is the transition energy and transition assignment. From our γ-ray spectra, the previously known decay scheme,[15] the (n,n′γ) reaction data,[16] and γ-ray decay systematics, the transitions observed in the present experiment were placed in the level diagram shown in Fig. 2. Most of the states in ^{191}Ir are grouped into three rotational-like bands based on the $\frac{3}{2}^+$ ground state, the $\frac{1}{2}^+$ first excited state, and the $\frac{7}{2}^+$ γ-vibrational-like state at 686.3 keV.

In addition to the positive parity states, several negative parity states appear to be Coulomb excited in ^{191}Ir with ^{136}Xe and ^{40}Ar ions. Complex spectra of unique-parity states in the odd-A Ir nuclei have been rather successfully described by the coupling of the $h_{11/2}$ hole to a rotating triaxial core by Meyer-ter-Vehn.[3] The $\frac{11}{2}^-$ state at 171 keV is not accessible by direct $E3$ excitation but the approximately equivalent γ-band head with $J=\frac{7}{2}^-$ at 391 keV is accessible by direct $E3$ and multiple excitation. There is also multiple $E2$ excitation within the negative parity states. Most of the 220 keV γ-ray intensity is attributed to the $\frac{7}{2}^-\rightarrow\frac{11}{2}^-$ transition. About 25% of the 220 keV γ-ray intensity is due to the impurity contribution ^{193}Ir $\frac{7}{2}\rightarrow\frac{5}{2}$ transition. A possible transition $\frac{5}{2}'\rightarrow\frac{5}{2}$ of 222 keV is too weak to contribute any intensity to the 220 keV peak, i.e., the intensity I_γ(222 keV) is only 3.5% of the I_γ(351 keV) $\frac{5}{2}'\rightarrow\frac{3}{2}$ transition[15] which corresponds to 6.1% of I_γ(220 keV).

The γ-ray yields were obtained from the peak areas and the Ge(Li) detector efficiencies. These efficiencies were determined with three different sources placed at the target position, viz., a National Bureau of Standards (NBS) mixed source (^{109}Cd, ^{139}Ce, ^{57}Co, ^{113}Sn, ^{137}Cs, ^{88}Y, and ^{60}Co), a NBS ^{152}Eu source, and a ^{226}Ra source. The γ-ray yields are presented relative to the $\frac{7}{2}^+\rightarrow\frac{3}{2}^+$ transition in Table I.

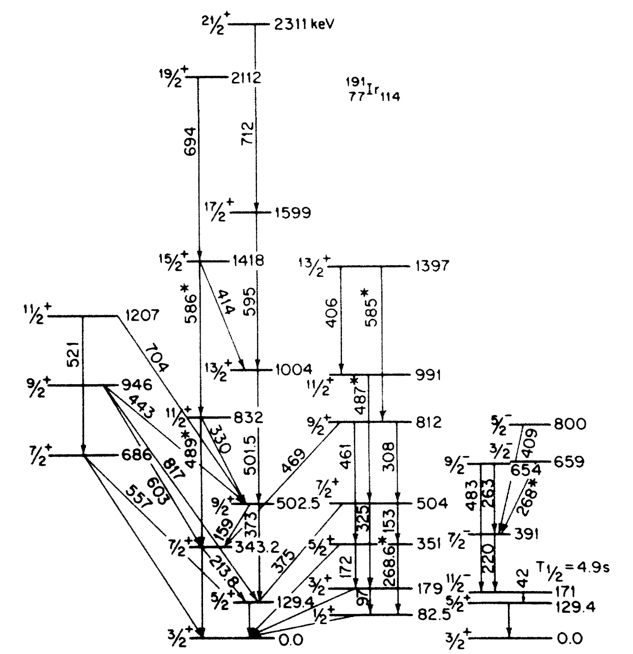

FIG. 2. Level diagram of states from Coulomb excitation and the γ-ray transitions from decay of these states. The transitions marked with an asterisk are placed more than once in the scheme.

III. DISCUSSION

We have compared the experimental γ-ray yields with the predictions of two models, viz., the particle-asymmetric-rigid-rotor model[14] and the IBFA model.[8] The Coulomb excitation yields are calculated using the Winther and de Boer[17] program which has been expanded to include $E1$, $E3$, and $E4$ excitations and augmented to provide integrated results over angle and energy by Sayer *et al.*[18] This computer program has also been expanded to handle up to 40 J states. For the input of the program, we use the experimental level energies and a set of $E2$ matrix elements. The latter, for example, were obtained from calculations using the particle-triaxial-rigid-rotor model program.[19] The $\frac{3}{2}^+$ [402] Nilson orbital (labeled by the sequence number 21 in the paper by Vieu *et al.*[14]), which has a large component $2d_{3/2}$, is the most likely orbital for the odd proton. This orbital accounts for the $\frac{3}{2}^+$, $\frac{1}{2}^+$, and $\frac{7}{2}^+$ bands. In the calculations the orbitals 20 and 19, corresponding mainly to $\frac{1}{2}^+$ [411] and $\frac{5}{2}^+$ [402] Nilsson orbitals which arise from the $2d_{3/2}$ and $2d_{5/2}$ shell model orbitals, were also included. The deformation parameters ϵ and γ were adjusted to give the best agreement between theoretical and experimental excitation energies. Figure 3 shows the γ dependence of the theoretical levels for $\epsilon=0.168$ and $E(2^+)=200$ keV alongside the experimental levels for ^{191}Ir. Levels with the symbols ○, +, and □ correspond to members of the $\frac{3}{2}^+$, $\frac{1}{2}^+$, and $\frac{7}{2}^+$ bands, respectively. The average absolute deviation between the experimental and theoretical energies is 45 keV for a fit to 20 states in ^{191}Ir with $\epsilon=0.168$, $\gamma=24.5°$, and

TABLE I. Relative γ-ray yields $\sum_{\theta_\gamma} I_\gamma(J_i \to J_f) / \sum_{\theta_\gamma} I_\gamma(\frac{7}{2} \to \frac{3}{2})$ for ^{191}Ir + 160-MeV ^{40}Ar and $I_\gamma(J_i \to J_f)/I_\gamma(\frac{7}{2} \to \frac{3}{2})$ for ^{191}Ir + 617-MeV ^{136}Xe. The unprimed, single-primed, and double-primed states refer to states in the $\frac{3}{2}^+$, $\frac{1}{2}^+$, and $\frac{7}{2}^+$ rotational-like bands, respectively.

J_i	J_f	E_γ (keV)	$\sum_{\theta_\gamma} I_\gamma(J_i \to J_f) / \sum_{\theta_\gamma} I_\gamma(\frac{7}{2} \to \frac{3}{2})$	$I_\gamma(J_i \to J_f)/I_\gamma(\frac{7}{2} \to \frac{3}{2})$
$\frac{21}{2}$	$\frac{17}{2}$	712		0.132±0.024
$\frac{19}{2}$	$\frac{15}{2}$	694		0.164±0.027
$\frac{17}{2}$	$\frac{13}{2}$	595	0.017±0.003	0.63 ±0.09
$\frac{15}{2}$	$\frac{11}{2}$	586	0.055±0.006	0.74 ±0.06
$\frac{15}{2}$	$\frac{13}{2}$	414	0.017±0.003	0.095±0.019
$\frac{13}{2}$	$\frac{9}{2}$	501	0.20 ±0.01	1.58 ±0.11
$\frac{11}{2}$	$\frac{7}{2}$	489	0.393±0.012	1.20 ±0.09
$\frac{11}{2}$	$\frac{9}{2}$	330	0.139±0.007	0.155±0.022
$\frac{9}{2}$	$\frac{5}{2}$	373	1.16 ±0.03	2.49 ±0.16
$\frac{9}{2}$	$\frac{7}{2}$	159	0.103±0.006	0.16 ±0.02
$\frac{7}{2}$	$\frac{3}{2}$	343	1.00	1.00
$\frac{7}{2}$	$\frac{5}{2}$	214	0.637±0.017	0.514±0.043
$\frac{5}{2}$	$\frac{3}{2}$	129	0.941±0.025	0.70 ±0.05
$\frac{13}{2}'$	$\frac{11}{2}'$	406		0.115±0.020
$\frac{11}{2}'$	$\frac{7}{2}'$	487	0.037±0.007	
$\frac{9}{2}'$	$\frac{5}{2}'$	461	0.055±0.005	0.190±0.025
$\frac{9}{2}'$	$\frac{7}{2}'$	308	0.030±0.004	0.103±0.016
$\frac{9}{2}'$	$\frac{7}{2}$	469	0.022±0.004	0.116±0.021
$\frac{7}{2}'$	$\frac{3}{2}'$	325	0.073±0.005	0.213±0.24
$\frac{7}{2}'$	$\frac{5}{2}'$	153	0.039±0.005	0.058±0.014
$\frac{7}{2}'$	$\frac{5}{2}$	375	0.038±0.008	
$\frac{5}{2}'$	$\frac{1}{2}'$	268	0.056±0.005	0.116±0.018
$\frac{5}{2}'$	$\frac{3}{2}'$	172	0.125±0.007	0.220±0.025
$\frac{5}{2}'$	$\frac{3}{2}$	351	0.105±0.006	0.196±0.024
$\frac{3}{2}'$	$\frac{1}{2}'$	97	0.065±0.013	
$\frac{3}{2}'$	$\frac{3}{2}$	179	0.044±0.004	0.098±0.020

TABLE I. (*Continued*).

J_i	J_f	E_γ (keV)	$\sum_{\theta_\gamma} I_\gamma(J_i \to J_f) / \sum_{\theta_\gamma} I_\gamma(\frac{7}{2} \to \frac{3}{2})$	$I_\gamma(J_i \to J_f)/I_\gamma(\frac{7}{2} \to \frac{3}{2})$
$\frac{11}{2}''$	$\frac{7}{2}''$	521	0.021 ± 0.003	0.127 ± 0.021
$\frac{11}{2}''$	$\frac{9}{2}$	704		0.080 ± 0.021
$\frac{9}{2}''$	$\frac{5}{2}$	817	0.017 ± 0.004	0.105 ± 0.025
$\frac{9}{2}''$	$\frac{7}{2}$	603	0.024 ± 0.004	0.221 ± 0.032
$\frac{9}{2}''$	$\frac{9}{2}$	443	0.020 ± 0.004	0.182 ± 0.025
$\frac{7}{2}''$	$\frac{3}{2}$	686	0.209 ± 0.009	0.400 ± 0.040
$\frac{7}{2}''$	$\frac{5}{2}$	557	0.276 ± 0.008	0.209 ± 0.025
$\frac{7}{2}^-$	$\frac{11}{2}^-$	220	0.045 ± 0.004	0.115 ± 0.024
$\frac{9}{2}^-$	$\frac{7}{2}^-$	263	0.019 ± 0.004	0.080 ± 0.015
$\frac{9}{2}^-$	$\frac{11}{2}^-$	483	0.024 ± 0.003	0.150 ± 0.024

$E(2^+)=200$ keV. These parameters are similar to those for the $(A-1)$ core ^{190}Os, viz., $\epsilon=0.157$, $\gamma=22.0°$, and $E(2^+)=187$ keV. Other parameters in this model calculation are the strength parameters κ_p and μ_p of the $l \cdot s$ and l^2 terms in the modified oscillator potential and the pairing strength parameters g_0 and g_1. The values of these parameters for the calculations presented in Fig. 3 were

$$\kappa_p=0.0620, \quad \mu_p=0.614\ ,$$

$$g_0=19.2 \text{ MeV}, \quad g_1=7.4 \text{ MeV}\ .$$

Finally, in the calculation of $B(M1)$ values, a gyromagnetic ratio scaling factor (GSFAC)=0.6 was applied to the value of the gyromagnetic ratio g_s for a free nucleon.

A striking feature of the level scheme is the doublet nature of the states J in the $\frac{3}{2}^+$ band and the states $J-1$ in the $\frac{1}{2}^+$ band. This characteristic feature also occurs in the IBFA Hamiltonian[20] when the odd fermion occupies two single particle orbits which differ in angular momentum by one unit, have equal single-particle energies, and have equal occupation probabilities. In this case the energy levels occur in doublets, differing in J by one unit, and corresponds to a pseudospin symmetry. The $2d_{3/2}$ and $3s_{1/2}$ levels in ^{191}Ir are close in energy and therefore the energy level spectra should approximate the pseudospin symmetry scheme.

The deformation parameters γ of the particle-asymmetric-rigid-rotor model is sharply defined in the fit to the states in the $\frac{7}{2}^+$ band. This contradicts most microscopic collective model calculations of potential energy surfaces which predict considerable γ softness (shallow deformation potentials). However, Leander pointed out in an earlier paper[10] that, where the core is actually quite soft, for example ^{186}Os and ^{187}Ir, the results can be quite similar to those obtained with a rigid core.

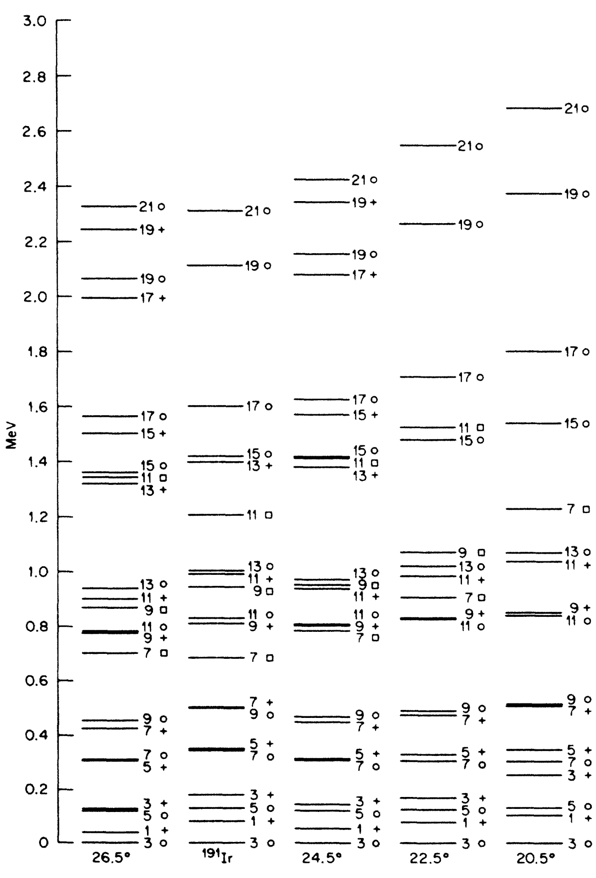

FIG. 3. Gamma dependence of the theoretical levels from the particle-triaxial-rigid-rotor model calculations for $\epsilon=0.168$ and $E(2^+)=200$ keV. Levels labeled with the symbols ○, +, and □ correspond to members of the $\frac{3}{2}^+$, $\frac{1}{2}^+$, and $\frac{7}{2}^+$ bands, respectively.

This choice of the above deformation parameters in the particle-triaxial-rigid-rotor model calculations reproduces the $B(E2)$ values deduced by Saladin *et al.*[21] from light-ion Coulomb excitation and from nuclear spectroscopic information[15] for the decay modes of the states in the $\frac{3}{2}^+$ band. A comparison of the experimental[15,21] and model-predicted $B(E2)$ values for ^{191}Ir is shown in Table II.

The input to the calculations of Coulomb excitation probabilities involved 38 states (23 positive-parity and 15 negative-parity states) and 173 $E2$ matrix elements (114 between the positive-parity states and 59 between the negative parity states). For the positive-parity states 15 of these $E2$ matrix elements were fixed by results deduced from light-ion Coulomb excitation[21] and nuclear spectroscopic information for the decay modes of these states. The remaining $E2$ matrix elements were taken from the triaxial-rotor model calculations. The $E2$ matrix elements between the negative-parity states were also obtained from the triaxial-rotor model calculations. In fact, the model predicts very collective $E2$ transitions between the negative-parity states with the deformation parameters deduced from the analysis of the positive-parity states. For these calculations, orbitals 19, 18, 17, and 16 were coupled to the asymmetric rotor. There orbitals correspond to the Nilsson orbitals $\frac{11}{2}^-$ [505], $\frac{9}{2}^-$ [514], $\frac{7}{2}^-$ [523], and $\frac{5}{2}^-$ [532], respectively. The 32 interband $E3$ matrix elements which connect the positive-parity and negative-parity states were chosen according to the Bohr-Mottelson collective vibrational model with the intrinsic transition matrix element taken to be 4 and 10 single particle units, respectively.

The $E2$ matrix elements from the IBFA model were also obtained from a numerical calculation. In the case of Spin(6) symmetry, the problem has been solved analytically.[12] This symmetry arises when the boson core has O(6) symmetry and the fermion occupies a single particle orbital with $j=\frac{3}{2}$. The numerical calculation[22] included only the $d_{3/2}$ orbital but did allow for breaking of the Spin(6) symmetry. This symmetry breaking was introduced in both the parameters of the boson core and the parameters of the boson-fermion interaction. The values of the parameters (ODDA code) used in the IBFA model calculations were

$$\text{pair}=0.0900\ \text{MeV},\quad PSD(1,1)=-0.1207\ \text{MeV}\ ,$$
$$ELL=0.0200\ \text{MeV},\quad PDD(1,1)=-0.6194\ \text{MeV}\ ,$$
$$QQ=0.0010\ \text{MeV},\quad PDD(3,1)=-0.0396\ \text{MeV}\ ,$$
$$OCT=0.0050\ \text{MeV},\quad EB=EF=0.1387\ e\,\text{b}\ .$$

All of the other parameters were set to zero. The form of the $T^{(E2)}$ operator[6,12] was taken to be

$$T^{(E2)}=EB[(d^\dagger\times\tilde{s}+s^\dagger\times\tilde{d})^{(2)}+\chi(d^\dagger\times\tilde{d})^{(2)}+(a^\dagger\times\tilde{a})^{(2)}]\ ,$$

where $s^\dagger$ (s) and $d^\dagger$ (d) denote the creation (annihilation) operators of the s and d bosons and $a^\dagger$ (a) denote creation (annihilation) operators for $J=\frac{3}{2}$ fermions. In the numerical calculations $\chi=-2.0$. The model-predicted $B(E2)$ values are listed in Table II for comparison with the experimental values. This model reproduces the $B(E2)$ values for the stronger (collective) transitions. However, it tends to underestimate the $B(E2)$ values for

TABLE II. Experimental and model-predicted $B(E2)$ values for ^{191}Ir.

Initial state		Final state			$B(E2,J_1\to J_j)$ $(e^2\text{b}^2)$		
J_i	K_i	J_f	K_f	E_γ (keV)	Experiment[a]	Triaxial rotor	Broken Spin(6) IBFA
$\frac{11}{2}$	$\frac{3}{2}$	$\frac{7}{2}$	$\frac{3}{2}$	489	0.469 ± 0.026[b]	0.524	0.527
$\frac{9}{2}$	$\frac{3}{2}$	$\frac{5}{2}$	$\frac{3}{2}$	373.1	0.663 ± 0.021[b]	0.513	0.485
$\frac{7}{2}$	$\frac{3}{2}$	$\frac{3}{2}$	$\frac{3}{2}$	343.2	0.278 ± 0.006	0.302	0.360
$\frac{7}{2}$	$\frac{3}{2}$	$\frac{5}{2}$	$\frac{3}{2}$	213.8	0.29 ± 0.04	0.173	0.268
$\frac{5}{2}$	$\frac{3}{2}$	$\frac{3}{2}$	$\frac{3}{2}$	129.4	0.598 ± 0.017	0.575	0.623
$\frac{5}{2}$	$\frac{3}{2}$	$\frac{1}{2}$	$\frac{1}{2}$	47.0	0.043 ± 0.022	0.078	0.020
$\frac{3}{2}$	$\frac{3}{2}$	$\frac{3}{2}$	$\frac{3}{2}$	0.0	0.331 ± 0.007[c]	0.137	0.451
$\frac{5}{2}$	$\frac{1}{2}$	$\frac{3}{2}$	$\frac{3}{2}$	351.1	0.020 ± 0.005	0.029	0.0035
$\frac{5}{2}$	$\frac{1}{2}$	$\frac{1}{2}$	$\frac{1}{2}$	268.6	≥0.58	0.316	0.313
$\frac{3}{2}$	$\frac{1}{2}$	$\frac{3}{2}$	$\frac{3}{2}$	179.0	0.108 ± 0.009	0.224	0.013
$\frac{3}{2}$	$\frac{1}{2}$	$\frac{1}{2}$	$\frac{1}{2}$	96.5	0.35 ± 0.07	0.213	0.249
$\frac{1}{2}$	$\frac{1}{2}$	$\frac{3}{2}$	$\frac{3}{2}$	82.5	0.136 ± 0.016	0.117	0.186
$\frac{7}{2}$	$\frac{7}{2}$	$\frac{3}{2}$	$\frac{3}{2}$	686.3	0.063 ± 0.002	0.023	0.0079
$\frac{7}{2}$	$\frac{7}{2}$	$\frac{5}{2}$	$\frac{3}{2}$	556.8	0.127 ± 0.022	0.091	0.223

[a]From Refs. 15 and 21 except if noted otherwise. Reference 15 also includes earlier Coulomb excitation results.
[b]From Ref. 21.
[c]From Ref. 28.

the less collective transitions by an order of magnitude, viz., the 351.1-, 179.0-, and 686.3-keV transitions. These transitions are forbidden in the Spin(6) symmetry as they have $\Delta\tau_1=2$. Inclusion of the $3s_{1/2}$ single particle orbital in the broken Spin(6) calculations is not expected to produce any major changes in the $E2$ matrix elements.[12,22] On the other hand, $M1$ matrix elements are dominated, to a large extent, by the single particle part of the $M1$ operator and are very sensitive to admixtures of other single particle orbitals.

Figure 4 shows a comparison between the experimental energy levels of ^{191}Ir and the theoretical levels from the IBFA model numerical calculations. The lowest representation of the Spin(6) symmetry for ^{191}Ir with $N=8$ bosons and $M=1$ fermions is $\sigma_1=N+\frac{1}{2}=\frac{17}{2}$. The numbers in parentheses denote the Spin(5) labels (τ_1,τ_2), where $\tau_2=\frac{1}{2}$ and $\tau_1=\sigma_1, \sigma_1-1, \ldots, \frac{1}{2}$ for $M=1$. All of the states of the lowest Spin(5) representations $(\frac{1}{2},\frac{1}{2})$, $(\frac{3}{2},\frac{1}{2})$, and $(\frac{5}{2},\frac{1}{2})$ are observed in ^{191}Ir by Coulomb excitation. Six of the eight states in the representation $(\frac{7}{2},\frac{1}{2})$ and four of the 11 states in the representation $(\frac{9}{2},\frac{1}{2})$ are also observed. The average absolute deviation between experimental and theoretical energies from the IBFA model calculations is 125 keV. The lines connecting the levels correspond to allowed collective transitions for which $\Delta\tau_1=\pm1$. The $\Delta\tau_1=0$ transitions are also allowed in the Spin(6) symmetry but are predicted to be less collective.

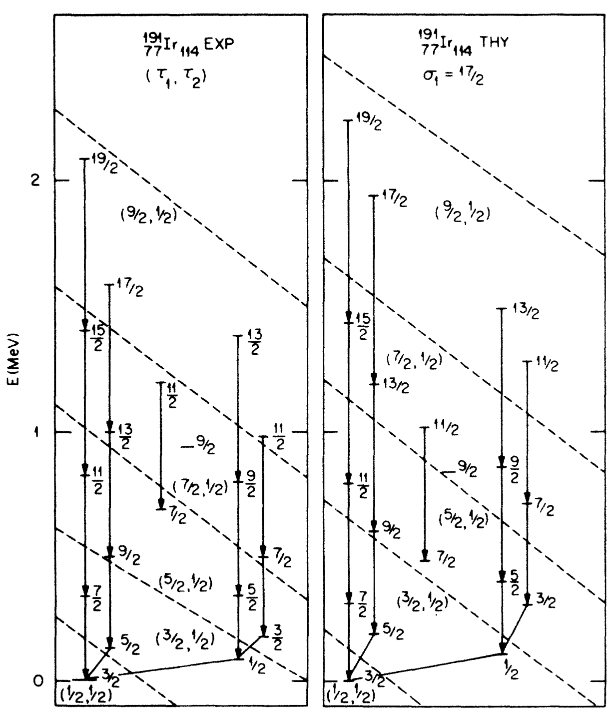

FIG. 4. Experimental level spectrum of ^{191}Ir and the theoretical levels from the IBFA model numerical calculations for the lowest representation of the Spin(6) symmetry. The numbers in parentheses denote the Spin(5) labels (τ_1, τ_2). The states of a given Spin(5) representation (τ_1, τ_2) are grouped between the dashed lines.

The Coulomb excitation yields were also calculated using $E2$ matrix elements obtained entirely from each model calculation. For transitions originating in the $K=\frac{1}{2}^+$ and $\frac{7}{2}^+$ bands, the experimental γ-ray yields are compared with model predictions from these calculations. This provides a more realistic test of the model predictions because the results from the light-ion Coulomb excitation of the $K=\frac{1}{2}^+$ and $\frac{7}{2}^+$ bands are not reproduced in detail by either model.

The Coulomb excitation calculations were done at three energies spanning the energy loss of the beam in the target. The statistical tensors were integrated over these energies. Following the Coulomb excitation process, the excited target nuclei are strongly aligned and recoil from the target into vacuum with a velocity $v/c\simeq2.7\%$ and in a highly ionized state. The interaction of the electronic fields of unpaired electrons with the nuclear moments causes a loss of alignment of the nuclear states with a corresponding attenuation of the angular distribution of the deexcitation γ rays. This vacuum depolarization effect was taken into account by using the measurements of Ben Zvi *et al.*[23] for ^{196,198}Pt. They found the interaction to be predominantly of a magnetic dipole and rapidly fluctuating character. In addition to the attenuation factors from the loss of nuclear alignment, the finite solid angle corrections for the γ-ray detectors were applied to the angular distribution functions. Also, a correction for the relativistic velocity transformation of the solid angle was applied to the statistical tensors. The γ-ray yield of a transition was calculated from the statistical tensors of the state which also included the contributions of the feeding from the levels above it. The branching ratios for decay of the states were calculated with the same $E2$ matrix elements used in the Coulomb excitation calculation and with $M1$ matrix elements taken from the model calculations. Internal conversion coefficients were obtained from the calculations of Rösel *et al.*[24] The sign and magnitude of the $E2/M1$ mixing ratio δ in the angular distribution functions were taken from the model calculations where

$$\delta^2=0.698E_\gamma^2\frac{B(E2)(e^2\mathrm{b}^2)}{B(M1)(\mu_N^2)} . \quad (1)$$

In order not to be exposed to errors in the calculated transition energy, the experimental value of E_γ in MeV was used.

Figure 5 shows the comparison of experimental γ-ray yields within the rotational-like band based on the $\frac{3}{2}^+$ ground state with the results from the model calculations for ^{191}Ir. The γ-ray yields are presented relative to the γ-ray yields for the $\frac{7}{2}^+\to\frac{3}{2}^+$ transition. The summation implies the sum of the yields observed at $\theta_\gamma=0°$, $55°$, and $90°$ for each transition. The overall agreement of both model predictions with the experimental results is quite good. Figure 6 shows the comparison between the experimental and calculated results for the transitions from decay of the $\frac{7}{2}^+$ state at 686.3 keV. Again the particle-asymmetric-rigid-rotor model predictions are in reasonable agreement with the data. In fact, this model prediction of $\delta=-1.1$ for the $\frac{7}{2}''\to\frac{5}{2}$ transition gives an excellent account of the observed angular distribution for this

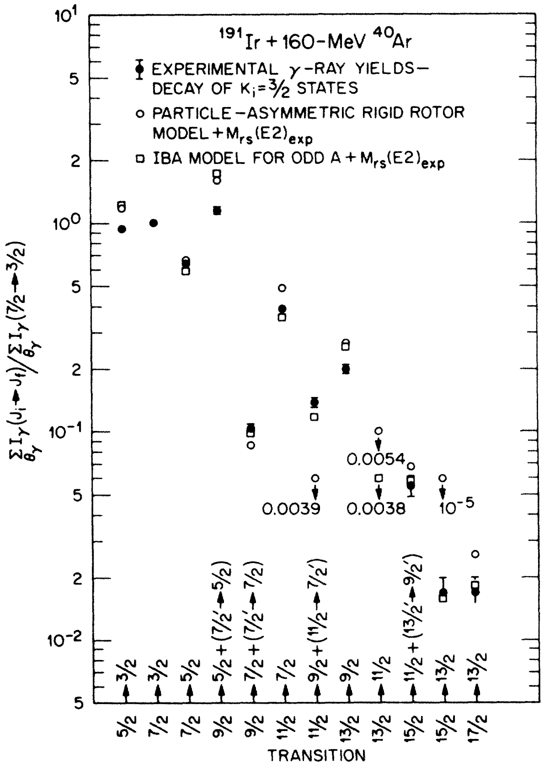

FIG. 5. Comparison of the experimental γ-ray yields with the results from the model calculations for transitions within the rotational-like band based on the $\frac{3}{2}^+$ ground state of ^{191}Ir.

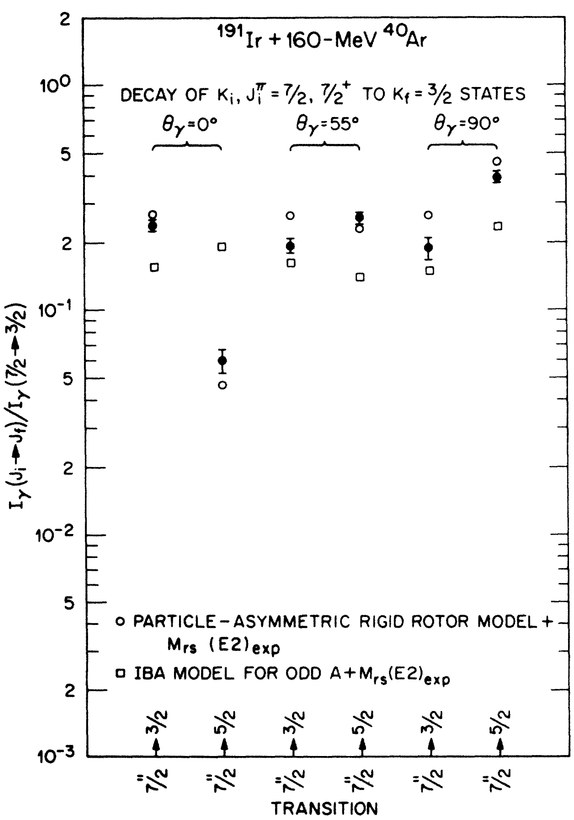

FIG. 6. Comparison of the experimental γ-ray yields with the results from the model calculations for transitions from the decay of the $\frac{7}{2}^+$ state at 686.3 keV in ^{191}Ir.

transition. However, the IBFA model predictions are in poor agreement with the data, viz., the model prediction of $\delta=23.6$ for the $\frac{7}{2}''\rightarrow\frac{5}{2}$ transition does not reproduce the observed angular distribution.

For transitions originating in the $K=\frac{1}{2}^+$ and $\frac{7}{2}^+$ bands, the experimental γ-ray yields are compared with the model predictions using $E2$ matrix elements entirely from the models. For transitions originating in the $K=\frac{1}{2}^+$ band, the overall agreement of the triaxial rotor model predictions with the experimental γ-ray yields is much better than the IBFA model predictions (see Fig. 7). The interband transition yields for the $\frac{3}{2}'\rightarrow\frac{3}{2}$, $\frac{5}{2}'\rightarrow\frac{3}{2}$, $\frac{7}{2}'\rightarrow\frac{5}{2}$, and $\frac{9}{2}'\rightarrow\frac{7}{2}$ are underestimated by 1 to 2 orders of magnitude by the IBFA model. These transitions originate in states with Spin(5) representations $(\frac{5}{2},\frac{1}{2})$ and $(\frac{7}{2},\frac{1}{2})$ and decay to states with Spin(5) representations $(\frac{1}{2},\frac{1}{2})$ and $(\frac{3}{2},\frac{1}{2})$ which are forbidden by the selection rule $\Delta\tau_1=2$ in the Spin(6) symmetry ($\Delta\tau_1=0,\pm 1$ are allowed). Also the $\frac{5}{2}'\rightarrow\frac{5}{2}$ transition (not shown in Fig. 7) is predicted to be strong with an intensity of 0.066 and is allowed in the Spin(6) symmetry but is not observed in the Coulomb excitation measurements. From the nuclear spectroscopic information[15] on the decay mode of this $\frac{5}{2}'$ state, the expected intensity in our Coulomb excitation measurements would have been 0.0036, which is too weak to be detected.

Neither model offers a satisfactory description of the γ-ray yields from decay of states in the $\frac{7}{2}^+$ rotational-like band (see Fig. 8). For example, the γ-ray yields for the transitions $\frac{7}{2}''\rightarrow\frac{3}{2}$ and $\frac{9}{2}''\rightarrow\frac{7}{2}$ are underestimated by

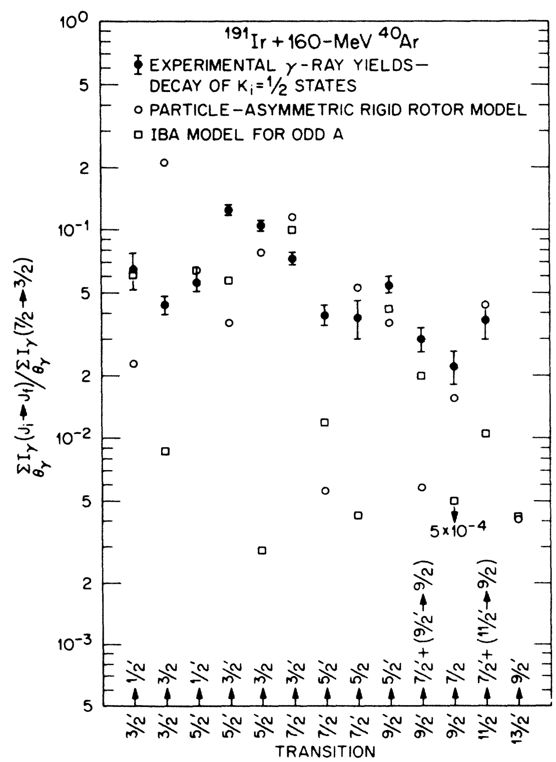

FIG. 7. Comparison of the experimental γ-ray yields with the results from the model calculations for the decay of states in the $\frac{1}{2}^+$ rotational-like band of ^{191}Ir.

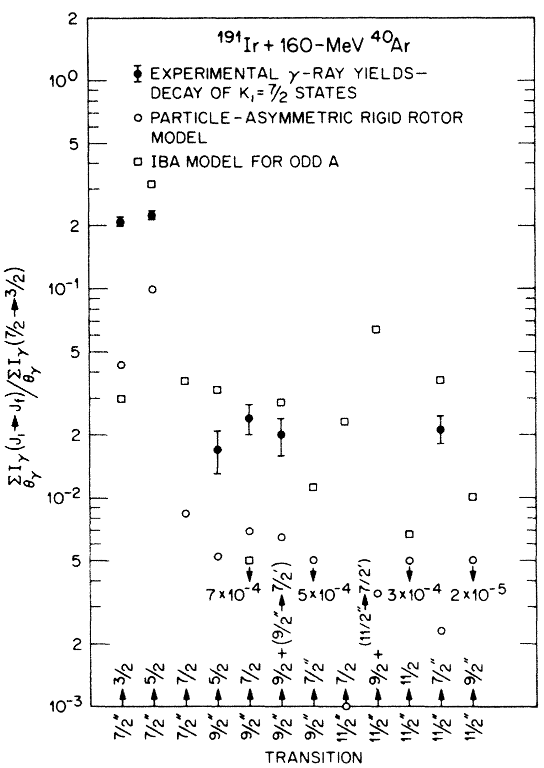

FIG. 8. Comparison of the experimental γ-ray yields with the results from the model calculations for the decay of states in the $\frac{7}{2}^+$ rotational-like band of ^{191}Ir.

both models. These transitions are forbidden by the (τ_1, τ_2) selection rule in the Spin(6) symmetry. Also the transitions $\frac{11}{2}''\to\frac{7}{2}$ and $\frac{11}{2}''\to\frac{9}{2}+\frac{11}{2}''\to\frac{7}{2}'$ are predicted to be strong by the IBFA model but are not observed. The $\frac{11}{2}''\to\frac{7}{2}$ transition is forbidden by the (τ_1,τ_2) selection rule but the energy dependence of the transition probability offsets the smallness of $E2$ matrix element. The other two transitions are allowed by the (τ_1,τ_2) selection rule; this and the energy dependence of the transition probability together lead to the large predicted yield. It is not at all clear whether the discrepancies with the IBFA model are related to the breakdown of Spin(6) symmetry or to the fact that some of the states observed in Coulomb excitation do not belong to the lowest representation of the Spin(6) symmetry. In this context, Iachello[11] and Iachello and Kuyucak[12] associated the $\frac{7}{2}''$ state at 686 keV with the representation $(\tau_1,\tau_2)=(\frac{5}{2},\frac{1}{2})$, which is the second $\frac{7}{2}$ state, whereas the experimental state is the third $\frac{7}{2}$ state in excitation energy. The third $\frac{7}{2}$ model state is in the representation $(\tau_1,\tau_2)=(\frac{7}{2}, \frac{1}{2})$. If the $\frac{7}{2}^+$ state at 686 keV is associated with this last model state, the deviations of the IBFA model predictions from the data are even larger. The predictions of the particle-asymmetric-rigid-rotor model consistently underestimate the γ-ray yields from decay of the states in the $\frac{7}{2}^+$ rotational-like band.

The $B(E3)$ for excitation of the negative-parity states extracted from the data is (4 ± 1) $B(E3)_{\mathrm{sp}}$. The inclusion of $E1$ matrix elements of 10^{-4} single particle units in the Coulomb excitation calculations did not change the $B(E3)$ value extracted from the data. The $B(E3)$ for excitation of the 3^- state at 1387 keV in ^{190}Os is (14 ± 2) $B(E3)_{\mathrm{sp}}$ where $B(E3)_{\mathrm{sp}}=1.5\times10^{-74}$ $e^2\mathrm{cm}^6$. This result was obtained from Coulomb excitation of ^{190}Os with 15-MeV ^{4}He ions. The amount of $E3$ strength fragmented into the low-lying states of ^{191}Ir is rather large.

IV. CONCLUSION

Prior to the present study, the experimental evidence (energy-level spectra,[12,13] electromagnetic transition probabilities,[12,13] and nuclear transfer reactions[25]) presented in support of U(6/4) supersymmetry in the Os-Ir nuclei has been limited. For example, only six $B(E2)$ values were known for ^{191}Ir. A far larger number of experimental data are needed before definite statements can be made about the occurrence of supersymmetry in these nuclei. From the present study, it can be concluded that the more collective transitions, viz., $\Delta\tau_1=1$ transitions of the Spin(6) symmetry, are described reasonably well by the IBFA model calculations with broken Spin(6) symmetry. On the other hand, there is one transition $\frac{3}{2}'\to\frac{3}{2}$ which is measured to be 17 $B(E2)_{\mathrm{sp}}$ but is a strictly forbidden $\Delta\tau_1=2$ transition in the Spin(6) symmetry. This collective $E2$ transition is not a special situation in ^{191}Ir but a general feature in ^{191}Ir, ^{193}Ir, and ^{197}Au.[26]

Since Spin(6) is contained as a subgroup of the chain decomposition of the U(6/4) supersymmetry, the results of Spin(6) symmetry can be used for the study of supersymmetry.[12] In this mass region the positive-parity single-particle orbitals for protons are $g_{7/2}$, $d_{5/2}$, $d_{3/2}$, and $s_{1/2}$. The U(6/4) supersymmetry scheme assumes that the proton moves only in the single-j orbital $d_{3/2}$. Since the $3s_{1/2}$ level is very near the $2d_{3/2}$ level, it would be of interest to test a more realistic multi-j supersymmetry scheme in which the $\frac{3}{2}'\to\frac{3}{2}$ transition, strictly forbidden in U(6/4) supersymmetry, might be allowed. Along this vein, Cizewski *et al.*[25] have considered the problem of perturbing the Spin(6) symmetry with terms which also couple the $s_{1/2}$ orbital with the even-even core. This perturbation reproduced the $d_{3/2}$ strength observed in the transfer reaction (t,α) on ^{194,196,198}Pt. However, with this perturbation one is no longer within the Spin(6) symmetry of a U(6/4) supersymmetry. As mentioned above, we do not expect major changes to occur in the $E2$ matrix elements with the inclusion of the $3s_{1/2}$ orbital. As an example, Iachello and Kuyucak[12] considered the modification introduced by the mixing of the $s_{1/2}$ orbital to the properties of the $\frac{1}{2}^+$ state at 73 keV in ^{193}Ir. For such a state the energy denominator of the perturbation treatment is small, i.e., the admixed amplitude is large. The effect of the mixing of the $3s_{1/2}$ orbital produced only a 23% reduction in the $B(E2,\frac{1}{2}\to\frac{3}{2})$. This transition in ^{193}Ir corresponds to the 82.5-keV transition in ^{191}Ir. In contrast the broken Spin(6) calculations without introduction of the $3s_{1/2}$ orbital produces a reduction of this $B(E2,\frac{1}{2}\to\frac{3}{2})$ by a factor of 2.4 from the Spin(6) symmetry calculations.

Very recently, Ling *et al.*[27] have developed the multi-j

supersymmetry scheme including all four positive parity single-particle orbitals, viz., U(6/20) supersymmetry. They found for many of the low-lying states in the lowest representation that the predictions of excitation energies are virtually identical in U(6/4) and U(6/20). Some $B(E2)$ values for the odd-A nucleus were also computed from the U(6/20) model.[27] In the U(6/20) supersymmetry scheme the quantum number $\sigma_1 = N + \frac{3}{2}$ for the lowest representation and in the U(6/4) supersymmetry scheme $\sigma_1 = N + \frac{1}{2}$ where N is the boson number in the odd-A nucleus. The selection rule $\Delta\tau_1$ for the $E2$ operator is the same in the U(6/20) and U(6/4) supersymmetry schemes of the odd-A nucleus. It should be noted that a simplified form was chosen for the $T^{(E2)}$ operator,[13,27] namely

$$T^{(E2)} = \gamma G^{(2)} , \tag{2}$$

where γ is an adjustable constant and $G^{(2)}$ is a generator of the group Spin(6). Table III presents a comparison between the experimental $B(E2)$ values and those computed using Eq. (2) for both U(6/20) and U(6/4). For completeness, the results from the IBFA model [broken Spin(6)] and the particle-asymmetric-rigid-rotor model calculations are included in Table III. The $B(E2)$ values

TABLE III. Comparison between experimental and model-predicted $B(E2)$ values for ^{191}Ir. The $B(E2)$ values are given in units of $B(E2)_{sp}$ and $B(E2)_{sp} = 0.006\,52$ e^2b^2 for $A = 191$. The adjustable parameter in Eq. (2) deduced from $B(E2)_{exp}$ for ^{190}Os is $\gamma^2 = 3.25$ $B(E2)_{sp}$. In U(6/20) $\sigma_1 = \frac{19}{2}$ and in U(6/4) $\sigma_1 = \frac{17}{2}$.

Nucleus	τ_{1i}	J_i	τ_{1f}	J_f	E_γ (keV)	$B(E2)_{exp}$	$B(E2)$ calculated U(6/20)	U(6/4)	Broken Spin(6)	Triaxial rotor
^{191}Ir	$\frac{3}{2}$	$\frac{1}{2}$	$\frac{1}{2}$	$\frac{3}{2}$	82.5	20.9± 2.4	82	68	28.5	17.9
	$\frac{3}{2}$	$\frac{5}{2}$	$\frac{1}{2}$	$\frac{3}{2}$	129.4	91.7± 2.6	82	68	95.6	88.2
	$\frac{3}{2}$	$\frac{7}{2}$	$\frac{1}{2}$	$\frac{3}{2}$	343.2	42.6± 0.9	82	68	55.2	46.3
	$\frac{5}{2}$	$\frac{3}{2}$	$\frac{1}{2}$	$\frac{3}{2}$	179.0	16.6± 1.4	0.0	0.0	2.0	34.4
	$\frac{5}{2}$	$\frac{5}{2}$	$\frac{1}{2}$	$\frac{3}{2}$	351.1	3.1± 0.8	0.0	0.0	0.5	4.4
	$\frac{5}{2}$	$\frac{7}{2}$	$\frac{1}{2}$	$\frac{3}{2}$	686.3	9.7± 0.3	0.0	0.0	1.2	3.5
	$\frac{3}{2}$	$\frac{5}{2}$	$\frac{3}{2}$	$\frac{1}{2}$	46.9	6.6± 3.4	12.3	10.3	3.1	12.0
	$\frac{3}{2}$	$\frac{7}{2}$	$\frac{3}{2}$	$\frac{5}{2}$	213.8	44.5± 6.1	18.0	15.1	41.1	26.5
	$\frac{5}{2}$	$\frac{3}{2}$	$\frac{3}{2}$	$\frac{1}{2}$	96.5	54 ±11	39	32	38.2	32.7
	$\frac{5}{2}$	$\frac{5}{2}$	$\frac{3}{2}$	$\frac{1}{2}$	268.6	≥ 89	67	55	48.0	48.5
	$\frac{5}{2}$	$\frac{7}{2}$	$\frac{3}{2}$	$\frac{5}{2}$	556.8	19.5± 3.4	57	46	34.2	14.0
	$\frac{5}{2}$	$\frac{9}{2}$	$\frac{3}{2}$	$\frac{5}{2}$	373.1	102 ± 3	88	72	74.4	78.7
	$\frac{5}{2}$	$\frac{11}{2}$	$\frac{3}{2}$	$\frac{7}{2}$	489.0	72 ± 4	111	91	80.8	80.4
$\sigma_{1i} = \frac{15}{2}$	$\frac{1}{2}$	$\frac{3}{2}$	$\frac{1}{2}$	$\frac{3}{2}$	539	(1.5± 0.7)[c]	0.0	0.0	0.02	5.6
$\sigma_{1i} = \frac{15}{2}$	$\frac{1}{2}$	$\frac{3}{2}$	$\frac{3}{2}$	$\frac{1}{2}$	457	0.6 ± 0.6	0.0	0.0	0.55	5.0
$\sigma_{1i} = \frac{15}{2}$	$\frac{1}{2}$	$\frac{3}{2}$	$\frac{3}{2}$	$\frac{5}{2}$	409	0.6 ± 0.3	0.0	0.0	0.09	3.8
$\sigma_{1i} = \frac{15}{2}$	$\frac{1}{2}$	$\frac{3}{2}$	$\frac{5}{2}$	$\frac{3}{2}$	360	0.5 ± 0.3	0.0	0.0	11.3	0.21
$\sigma_{1i} = \frac{15}{2}$	$\frac{1}{2}$	$\frac{3}{2}$	$\frac{5}{2}$	$\frac{5}{2}$	188	$2.4^{+13}_{-1.8}$	0.0	0.0	4.0	2.4
	$\frac{1}{2}$	$\frac{3}{2}$	$\frac{1}{2}$	$\frac{3}{2}$	0.0	(50.8 ± 1.1)[a]	85	71	69	21.0
^{190}Os	1	2	0	0	186.7	(76.0 ± 0.6)[b]				

[a]Reference 28.
[b]Reference 29.
[c]References 15, 21, and 30. Gamma-ray branching ratios and $E2/M1$ ratios for decay of the 539-keV state are taken from Refs. 15 and 30.

predicted by U(6/20) and U(6/4) supersymmetry schemes differ by only about 20%. For both supersymmetry schemes there is a lack of detailed agreement with the $B(E2)$ values for the $\Delta\tau_1=1$ transitions from the decay of the $\tau_1=\frac{3}{2}$ states to the $\frac{3}{2}$ ground state. These features are, however, reproduced to a much better degree by the broken Spin(6) calculation. There are six observed $\Delta\tau_1=2$ transitions with moderately collective $B(E2)$'s which are strictly forbidden in these supersymmetry schemes. The broken Spin(6) calculations also disagree with the data for the $\Delta\tau_1=2$ transitions, i.e., the predictions range between 2.0 and 0.09 $B(E2)_{\text{sp}}$. By far the most successful interpretation of the experimental energies of the states and the $B(E2)$ values in ^{191}Ir is the particle-asymmetric-rigid-rotor model.

Because of the simple form chosen for the $E2$ transition operator, only small differences in the $B(E2)$ values are predicted by the U(6/20) and U(6/4) supersymmetry schemes. It remains to be seen if a more general form of the $E2$ transition operator would improve the description of the $B(E2)$ values in ^{191}Ir, in particular, a relaxation of the forbidden $\Delta\tau_1=2$ transitions. Different degrees of freedom, as in the triaxial rotor, are probably needed to describe the energy-level spectrum of ^{191}Ir.

There are several other positive parity states[15] known in ^{191}Ir which were not observed in our heavy-ion Coulomb excitation measurements, viz., 539 keV ($\frac{3}{2}$), 588 keV ($\frac{5}{2}$), 624 keV ($\frac{1}{2}$ or $\frac{3}{3}$), 748 keV ($\frac{5}{2}$), and 763 keV ($\frac{3}{2}$). Upper limits of the $B(E2)$'s for excitation of these states could be obtained from direct $E2$ Coulomb excitation with ^{4}He ions. In the $\sigma_1=\frac{17}{2}$ representation there are several low spin states which have not been exhausted. These are $\frac{5}{2}$ and $\frac{3}{2}$ in the representation $(\frac{7}{2},\frac{1}{2})$ and $\frac{9}{2}$, $\frac{7}{2}$, $\frac{7}{2}$, and $\frac{5}{2}$ in the representation $(\frac{9}{2},\frac{1}{2})$. However, Iachello and Kuyucak[12] have associated the third $\frac{3}{2}^+$ state at 539 keV in ^{191}Ir with the $\sigma_1=\frac{15}{2}$, $\tau_1=\frac{1}{2}$ representation. The lifetime of the 539-keV state is known from ^{191}Ir(γ,γ) resonance fluorescence.[15] For completeness the $B(E2)$'s from the decay of this state are included in Table III. These $B(E2)$'s are forbidden in the U(6/20) and U(6/4) and supersymmetry schemes as they have $\Delta\sigma_1=1$ ($T^{(E2)}$ operator satisfies the selection rule $\Delta\sigma_1=0$). In the triaxial rotor model the main component in the wave function of the third $\frac{3}{2}^+$ state comes from the $\frac{1}{2}^+$ [411] Nilsson orbital which arises from the $2d_{3/2}$ shell model orbital.

ACKNOWLEDGMENTS

We are indebted to F. Iachello for numerous discussions concerning the IBFA model, spinor symmetries, and supersymmetries and to F. Iachello and S. Kuyucak for the broken Spin(6) calculations of energies, $E2$, and $M1$ matrix elements. We are extremely grateful to G. Leander for discussions and for supplying the code for the particle-asymmetric-rigid-rotor model, to W. B. Ewbank for discussions on the use of this program, to J. Saladin for communicating the $B(E2)$ values from light-ion Coulomb excitation which were used in the calculation of Coulomb excitation yields, and to A. Balantekin for stimulating discussions. Finally, we wish to thank R. Sayer for expanding the Winther-de Boer code to handle 40 J states. Oak Ridge National Laboratory is operated by Martin Marietta Energy Systems, Inc. for the U.S. Department of Energy under Contract No. DE-AC05-840R21400. Research at the University of Tennessee is supported by U.S. Department of Energy under Contract No. DE-AS05-76ER04936. Research at the Lawrence Berkeley Laboratory is supported by U.S. Department of Energy under Contract No. DE-AC03-76SF00098.

*Present address: Etudes et Productions, Schlumberger, Clamar, France.

†Present address: Department of Physics, University of Jyväskylä, SF-40720 Jyväskylä 72, Finland.

‡Present address: Department of Nuclear Physics, Australian National University, Canberra ACT 2601, Australia.

[1] K. Kumar and M. Baranger, Nucl. Phys. **A122**, 273 (1968).

[2] I. Y. Lee, D. Cline, P. A. Butler, R. M. Diamond, J. O. Newton, R. S. Simon, and F. S. Stephens, Phys. Rev. Lett. **39**, 684 (1977).

[3] J. Meyer-ter-Vehn, Nucl. Phys. **A249**, 111 (1975); **A249**, 141 (1975).

[4] A. Arima and F. Iachello, Ann. Phys. (N.Y.) **99**, 253 (1976).

[5] A. Arima and F. Iachello, Ann. Phys. (N.Y.) **111**, 201 (1978).

[6] A. Arima and F. Iachello, Ann. Phys. (N.Y.) **123**, 468 (1979).

[7] A. Bohr and B. R. Mottelson, *Nuclear Structure* (Benjamin, Reading, Mass., 1975), Vol. II.

[8] F. Iachello and O. Scholten, Phys. Rev. Lett. **43**, 679 (1979).

[9] F. Iachello, Nucl. Phys. **A347**, 51 (1980).

[10] G. Leander, Nucl. Phys. **A273**, 286 (1976).

[11] F. Iachello, Phys. Rev. Lett. **44**, 772 (1980).

[12] F. Iachello and S. Kuyucak, Ann. Phys. (N.Y.) **136**, 19 (1981).

[13] A. B. Balantekin, I. Bars, and F. Iachello, Nucl. Phys. **A370**, 284 (1981).

[14] Ch. Vieu, S. E. Larsson, G. Leander, I. Ragnarsson, W. De Wieclawik, and J. S. Dionisio, Z. Phys. A **290**, 301 (1979).

[15] E. Browne, Nucl. Data Sheets **30**, 653 (1980).

[16] E. W. Kleppinger and S. W. Yates, Bull. Am. Phys. Soc. **29**, 1049 (1984); E. W. Kleppinger, Ph.D. thesis, University of Kentucky, 1984.

[17] A. Winther and J. de Boer, in *Coulomb Excitation,* edited by K. Alder and A. Winther (Academic, New York, 1966), p. 303.

[18] R. O. Sayer, P. H. Stelson, F. K. McGowan, W. T. Milner, and R. L. Robinson, Phys. Rev. C **1**, 1525 (1970).

[19] S. E. Larsson, G. Leander, and I. Ragnarsson, Nucl. Phys. **A307**, 189 (1978). Computer code supplied by G. Leander.

[20] O. Scholten, Phys. Lett. **108B**, 155 (1982).

[21] J. X. Saladin, A. A. E. Hussein, C. Y. Chen, S. Sergiwa, and C. Kuo, Bull. Am. Phys. Soc. **27**, 705 (1982); A. A. E. Hussein, Ph.D. thesis, University of Pittsburgh, 1981.

[22] The results from the IBFA model calculations were supplied by Iachello and Kuyucak.

[23] I. Ben Zvi, P. Gilad, M. Goldberg, G. Goldring, A. Schwarzschild, A. Sprinzak, and Z. Vager, Nucl. Phys. **A121**, 592 (1968).

[24] R. Rösel, H. M. Fries, K. Alder, and H. C. Pauli, At. Data Nucl. Data Tables **21**, 291 (1978).

[25]J. A. Cizewski, D. G. Burke, E. R. Flynn, R. E. Brown, and J. W. Sunier, Phys. Rev. C **27**, 1040 (1983).

[26]F. K. McGowan, W. T. Milner, R. L. Robinson, and P. H. Stelson, Ann. Phys. (N.Y.) **63**, 549 (1971).

[27]Yin-Sheng Ling, Mei Zhang, Jing-Ming Xu, Michel Vallieres, Robert Gilmore, Da Hsuan Feng, and Hong-Zhou Sun, Phys. Lett. **148B**, 13 (1984).

[28]Y. Tunaka, R. M. Steffen, E. B. Shera, W. Reuter, M. V. Hoehn, and J. D. Zumbro, Phys. Rev. Lett. **51**, 1633 (1983).

[29]M. V. Hoehn, E. B. Shera, H. D. Wohlfahrt, Y. Y. Yamazaki, R. M. Steffen, and R. K. Sheline, Phys. Rev. C **24**, 1667 (1981).

[30]K. S. Krane, At. Data Nucl. Data Tables **18**, 137 (1976).